



Nanocrystalline Mixed Ligand Complexes of Cu (II), Ni (II), Co(II) with N, O Donor Ligands: Synthesis, Characterization, and Antimicrobial Activity

KOLHE NITIN H¹, JADHAV SHRIDHAR S^{1*}, SHAIKH SAJID H²,
TAKATE SUSHAMA J¹ and AWARE DINKAR V³

¹P.G. Department of Chemistry and Research Centre, New Arts Commerce and Science College Ahmednagar; Affiliated to Savitribai Phule Pune University Lal-taki Rd -414401, Ahmednagar (M.S.) India.

²P.G. Department of Microbiology, New Arts Commerce & Science College, Ahmednagar, India.

³Department of Chemistry, Arts, Commerce and Science College Sonai, Tal-Newasa, Dist.-Ahmednagar -414603, Affiliated to S.P. Pune University, India.

*Corresponding author E-mail: ssjadhav1957@gmail.com

<http://dx.doi.org/10.13005/ojc/320620>

(Received: September 06, 2016; Accepted: October 10, 2016)

ABSTRACT

In present investigation nanocrystalline mixed ligand complexes were synthesized using 8-hydroxyquinoline, salicylaldehyde with metals like Cu (II), Ni (II) and Co (II). The metal: ligand ratio was found to be 1:1:1. These complexes were characterized using electronic spectra, FTIR spectra, elemental analysis, magnetic susceptibility, thermogravimetric analysis, conductivity measurement, powder X-ray diffraction and Scanning Electron Microscopy with electron dispersive spectroscopic methods. The electronic spectra of complexes suggest that they have square planar geometries. In FTIR analysis characteristic bands of ν (M-N) and ν (M-O). The Co (II) and Cu (II) complexes are paramagnetic in nature and these had square planar geometry. While Ni (II) complexes are diamagnetic nature and having square planar geometry. The thermal analysis of complexes was studied in an attempt to assign intermediate compounds. Low molar conductance values indicate non – electrolytic nature of the complexes. The Powder X-ray diffraction study shows formation of nanocrystalline phase as well as the grain size of complexes is less than 10 nm. The EDS study is shows good agreement for formation of mixed ligand metal complexes. Complex: $[C_{16}H_{12}CuN_2O_2]$, $[C_{14}H_{12}Ni_2NiO_4]$, $[C_{16}H_{12}NiN_2O_2]$ and $[C_{16}H_{12}CoN_2O_2]$ had antimicrobial activity against four bacteria tested. Bacteria were resistant to other five complexes.

Keywords: Nanocrystalline complexes, N, O donor, SEM-EDS, Disc Diffusion.

INTRODUCTION

A lot of attention is being given on the study of simple transition metal complexes and their biological activity¹. The N, O donor ligands

have been used as chelating agents in the field of coordination chemistry and medicine. The importance of N, O donor ligands and their metal complexes in different biological activities is very well known². These biological activities include

anti-inflammatory, antimicrobial, anticancer and antidermal activity. They are also studied as enzyme inhibitors. Cis-platin is one of the best examples of mixed ligand complex^{3,4}. The Nano crystalline quantum dot mixed ligands complexes play an important role in inorganic, organometallic chemistry and medicinal chemistry. A lot of research has been carried out on synthesis and characterization of mixed ligand transition metal complexes⁵⁻⁶. But till date nanocrystalline complexes of transition metal ion have been given very little attention. Therefore study of nanocrystalline mixed ligand transition metal complexes has a great scope in the field of research in inorganic chemistry. Due to the change in their physical properties, such as surface area, decomposition temperature, magnetic properties, these nanocrystalline metal complexes can be used as catalyst in organic synthesis. Considering all above facts the aim of current research is synthesis and characterization of nanocrystalline mixed ligand complexes of Co (II), Ni(II) and Cu (II) with N,O donors and study of their antimicrobial activity.

EXPERIMENTAL

Chemicals

AR grade metal salts of NiCl₂.6H₂O, CuCl₂.2H₂O and CoCl₂.6H₂O were purchased from Loba chemicals. The salicylaldehyde and 8-hydroxyquinoline, ethanol, potassium hydroxide were purchased from Merck chemicals.

General procedure for synthesis of complexes Ni(II), Cu(II) and Co (II) ions with salicylaldehyde ligands

1 mmole of salicylaldehyde was dissolved in alcoholic KOH. This solution was added drop wise to the solution of 1mmole metal salts in alcohol. The reaction mixture was refluxed for appropriate time. The solid product was obtained after completion of the reaction. The Co (II) with ligand reaction was kept in inert atmosphere and solution was bubbled with nitrogen gas for 10 minutes. All the complexes of salicylaldehyde with Ni(II), Cu(II) ions and Co (II) were synthesized by reported methods⁷.

General Procedure for Synthesis of complexes of N, O (8-Hydroxyquinoline) donors with Ni (II), Cu (II) and Co(II) ions

The ligand 8-Hydroxyquinoline with Ni (II),

Cu (II) and Co (II) ions was synthesized by modifying literature methods⁸. 1mmole of 8-hydroxyquinoline was dissolved in alcoholic KOH. This solution was added drop wise to the solution of 1mmole metal salt in alcohol. The reaction mixture was refluxed for appropriate time. The solid product was obtained after completion of the reaction.

Synthesis of mixed ligand complexes of 8-hydroxyquinoline and salicylaldehyde with Ni (II), Cu (II) and Co (II) metal ions

1mmole of metal salts was dissolved in alcohol. To this 1mmole of 8-hydroxyquinoline and 1mmole of salicylaldehyde in alcoholic KOH were added respectively with constant stirring. The mole ratio of M :L₁:L₂ was 1:1:1 and reaction mixture was refluxed for 6 hrs. In synthesis of Co (II) complex the reaction was carried out in inert atmosphere to prevent the oxidation of Co(II). The reaction mixture was evaporated to about half of the original volume which on cooling afforded the solid product. The product was filtered, washed with cold dry ethanol and dried in vacuum.

Antimicrobial activity of Complexes and Ligands

The antimicrobial activities of ligand as well as complexes were tested by agar disc diffusion method using Mueller Hinton Agar (MHA)^{9,10}. Antimicrobial activity of each complex was tested for *Bacillus subtilis* NCIM 2063 and *Escherichia coli* NCIM 2341. The MHA was prepared and poured in the plates after sterilization. The plates were allowed to solidify for 15 minutes. Sterile 5mm Whatmann filter paper disc was loaded with test compounds (100µg/disc) and placed over inoculated plates. The dimethylsulfoxide (DMSO) was kept as negative control¹¹. The plates were then incubated at 37°C for 24h. After incubation the plates were observing for zones of inhibition. The diameter of zones of inhibition was recorded for the positive plates.

Physical Measurements and analysis

The FTIR spectra of complexes were obtained on Shimadzu IRAffinity-1 Fourier transform Infrared spectrophotometer on samples pressed on KBr pellets. UV-Vis absorption measurements were carried out on a Shimadzu UV1800 at 26°C in 10⁻³ in DMF and DMSO. The Elemental analysis (C, H, and N) was done by using PerkinElmer

analyzer. Magnetic properties were determined from Gouy balance method. The thermogravimetric analysis was carried out on Shimadzu TGA50H thermoanalyzer. The synthesized nanocrystalline powders were characterized by various sophisticated techniques such as powder X-ray diffraction (XRD) patterns recorded on a model Philips X-ray diffractometer with diffraction angle 2θ in between 20° to 80° using Cu-K α radiation of wavelength 1.54058 Å. The grain size was calculated from grain size programmer software by using the XRD data such as FWHM, wavelength of Cu-K α radiation. The Surface morphology and elemental analysis of the samples were carried out using scanning electron microscopy with electron dispersion spectroscopy (SEM-EDS) characterization conducted using a JEOL-JEM -6360A Analytical scanning Electron Microscope(Oxford).

RESULTS AND DISCUSSION

The elemental analysis data, decomposition temperature, colour, mol. wt., percentage yield and molar conductance were given in Table 1.

Infrared Spectroscopy

The FTIR spectra provide valuable information on the nature of the functional group attached to the metal atom. The characteristic IR frequencies of ligand 8-hydroxyquinoline (L_1) [C_9H_7NO], salicylaldehyde (L_2) [$C_7H_7NO_2$] and their complexes were described in Table 2. The FTIR Spectrum of C_9H_7NO (L_1) shows the frequency 3300-3340 cm^{-1} is attributed to the phenolic OH group. The frequency 1412 cm^{-1} attributed to C=N in the ring¹² and the N-H frequency 3300-3600 cm^{-1} . The infrared spectrum of the [$C_7H_7NO_2$] ligand showed strong and broad band's due to the hydrogen bonded phenolic OH at O-position in the region 3000–2800 cm^{-1} . It also exhibits two separate OH bands of the oxime OH at 3237 cm^{-1} and 3137 cm^{-1} and phenolic OH at 3400 cm^{-1} . The dwarf bands observed in the 1646–1620 cm^{-1} frequency ranges of the complexes were assigned to the $\nu(C=N)$.¹³ The shift of the $\nu(C=N)$ vibration in all the complexes to a lower frequency suggests that the nitrogen atom of the ring contributes to the complexation. The lower $\nu(C=N)$ frequency also indicates stronger M–N co-ordination bonding. In the IR spectra of the complexes, a band was observed between 403 cm^{-1} and 476 cm^{-1} ,

which is attributed to $\nu(M-N)$ stretching vibrations.¹⁴ Another band appeared between 493 cm^{-1} and 619 cm^{-1} , which are assigned to the interaction of the phenolic oxygen to the metal atom.

In all the Cu(II) metal ligand complexes, a band appear in the range of 403 cm^{-1} to 476 cm^{-1} is attributed to $\nu(Cu-N)$.¹⁵⁻¹⁶ In case of [$C_{18}H_{12}CuN_2O_2$] shows 403 cm^{-1} , while [$C_{14}H_{12}CuN_2O_4$] shows 476 cm^{-1} . The complex [$C_{16}H_{12}CuN_2O_3$] shows $\nu(Cu-O)$ frequency at 466 cm^{-1} is in between the [$C_{18}H_{12}CuN_2O_2$] and [$C_{14}H_{12}CuN_2O_4$] indicate the formation of the mixed ligand complex. The $\nu(Cu-N)$ for the complexes [$C_{18}H_{12}CuN_2O_2$], [$C_{14}H_{12}CuN_2O_4$] and [$C_{16}H_{12}CuN_2O_3$] is 596 cm^{-1} , 525 cm^{-1} and 518 cm^{-1} , respectively. This observation is similar to that of $\nu(Cu-O)$ for all the copper complexes. Similarly the $\nu(C=C)$ and $\nu(C-O)$ for these complexes were at 1446 cm^{-1} , 1469 cm^{-1} , 1475 cm^{-1} and 1545 cm^{-1} , 1139 cm^{-1} , 1597 cm^{-1} respectively. The frequency of ligand [C_9H_7NO] shows 1500 cm^{-1} and 1215 cm^{-1} is attributed to $\nu C=C$ and $\nu C-O$ respectively. The decreased frequency in Cu (II)-Ligands complex by 54 cm^{-1} to 25 cm^{-1} and 76 cm^{-1} units indicates formation of complex.

In case of [$C_{14}H_{12}NiO_4$], [$C_{18}H_{12}NiN_2O_2$] and [$C_{16}H_{12}NiN_2O_3$] complexes, the bands at 426 cm^{-1} , 450 cm^{-1} , 465 cm^{-1} and 508 cm^{-1} , 505 cm^{-1} and 504 cm^{-1} were attributed to $\nu(Ni-N)$ and $\nu(Ni-O)$ bond formation between ligands and metal ion. The bands at 3059 cm^{-1} , 3062 cm^{-1} were attributed to aromatic $-C=C-$ and 2955 cm^{-1} were attributed to $\nu(-C-H)$, Ni(II)-L complexes. The $\nu(C-O)$ and $\nu(C=N)$ frequencies observed to be decreased in complexes by 56 cm^{-1} and 90 cm^{-1} respectively as compared with ligands. Mainly the frequency of mixed ligands complexes shows the intermediate frequency between the metal complexes.

In case of all the three complexes of Co(II), $\nu(Co-O)$, $\nu(Co-N)$, $\nu(C=N)$, (C-O-) bands were observed at 410 cm^{-1} , 462 cm^{-1} , 450 cm^{-1} , 493 cm^{-1} , 505 cm^{-1} , 619 cm^{-1} , 1545 cm^{-1} , 1542 cm^{-1} , 1639 cm^{-1} , 1469 cm^{-1} , 1423 cm^{-1} , 1420 cm^{-1} respectively.

Electronic Spectra

The electronic spectra are shown in fig.1 for ligands and their metal complexes. The ligand

Table1: Physical Characteristics and Analytical data for ligands and their metal complexes

Sr. No.	Complexes	Color	Mol. Wt.	M.P °C	Yield %	C	H	O	N	Molar Conductance $\Omega^{-1}\text{cm}^2\text{mol}^{-1}$
L ₁	[C ₉ H ₇ NO]	White	145.15	74	---	---	---	---	---	---
L ₂	[C ₇ H ₇ NO ₂]	White	137.13	58	---	---	---	---	---	---
1	[C ₁₄ H ₁₂ CuN ₂ O ₄]	Yellowish Green	335.80	246d*	74.55%	50.07(49.80)	3.00(2.97)	19.76(19.68)	8.34(8.33)	06.30
2	[C ₁₈ H ₁₂ CuN ₂ O ₂]	Faint Green	351.84	256d*	71.21%	61.45(61.39)	3.44(3.30)	9.09(9.10)	7.96(7.89)	09.60
3	[C ₁₆ H ₁₂ CuN ₂ O ₃]	Green	343.83	>300d*	68.00%	55.89(55.81)	3.52(3.27)	13.16(12.98)	8.15(8.11)	03.75
4	[C ₁₄ H ₁₂ N ₂ NiO ₄]	Greenish Yellow	330.94	135d*	67.34%	50.81(50.54)	3.65(3.64)	19.34(19.32)	8.46(8.44)	07.35
5	[C ₁₈ H ₁₂ NiN ₂ O ₂]	Green	346.99	263d*	53.00%	62.30(62.28)	3.49(3.48)	9.22(9.22)	8.07(8.07)	07.70
6	[C ₁₆ H ₁₂ NiN ₂ O ₃]	Dark olive Green	338.97	230d*	65.63%	56.69(56.63)	3.57(3.49)	14.16(13.69)	8.16(8.07)	09.26
7	[C ₁₄ H ₁₂ CoN ₂ O ₄]	Radish Brown	331.18	>305d*	58.06%	56.20(56.18)	4.04(4.04)	10.70(10.68)	9.36(9.30)	01.90
8	[C ₁₈ H ₁₂ CoN ₂ O ₂]	Brown	347.23	>300d*	59.93%	62.26(62.24)	3.48(3.47)	9.22(9.19)	8.07(8.05)	01.65
9	[C ₁₆ H ₁₂ CoN ₂ O ₃]	Chocolate Brown	339.21	290d*	57.74%	56.65(56.62)	3.57(3.55)	14.15(14.10)	8.26(8.11)	03.75

d* = Decomposition temperature.

band D for L_1 : $[C_9H_7NO]$ and band B for L_2 : $[C_7H_7NO_2]$ shows two absorption bands at 245nm, 275nm and 247nm, 265nm, respectively. However, it appears reasonable to assign the bands $\pi \rightarrow \pi^*$ transitions due to δ -bonded electron and $\pi \rightarrow \pi^*$ due to non-bonded pair of the electron on the oxygen atom respectively¹⁷.

The two bands were observed for heteroleptic complex of copper such as I: $[C_{16}H_{12}CuN_2O_3]$ (Fig. 1). These bands were assigned with ${}^2B_{2g} \rightarrow {}^2B_{1g}$

and ${}^2E_g \rightarrow {}^2B_{1g}$ transition at 575nm and 478nm respectively. These transitions indicate the geometry of complex is square planar¹⁹. It was also supported by magnetic susceptibility measurement. The other two homoleptic complex G: $[C_{18}H_{12}CuN_2O_2]$, H: $[C_{14}H_{12}CuN_2O_4]$ shows absorption at 415nm and 500nm, at 345nm and 525nm respectively.

Complex F: $[C_{16}H_{12}NiN_2O_2]$ exhibited three bands at 623nm, 428nm and 224nm. Which was attributed to the ${}^3A_{2g} \rightarrow {}^3T_{2g}(F)$ (ν_1); ${}^3A_{2g} \rightarrow {}^3T_{1g}(F)$

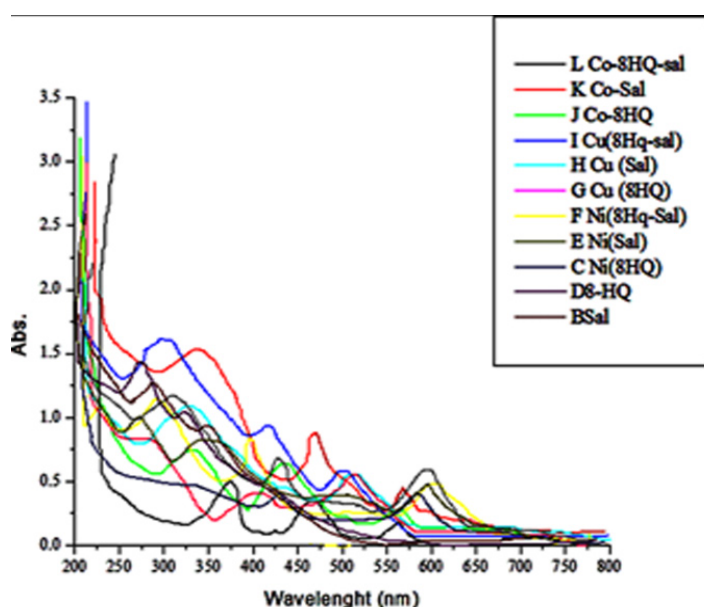


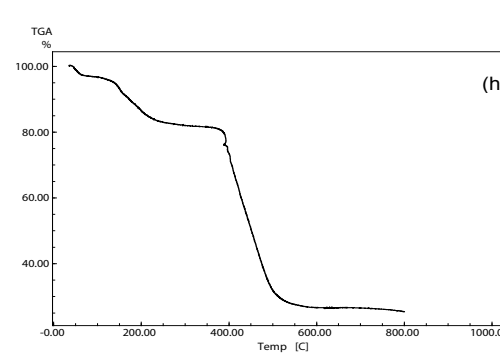
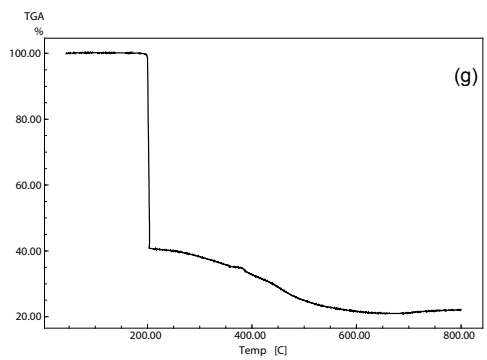
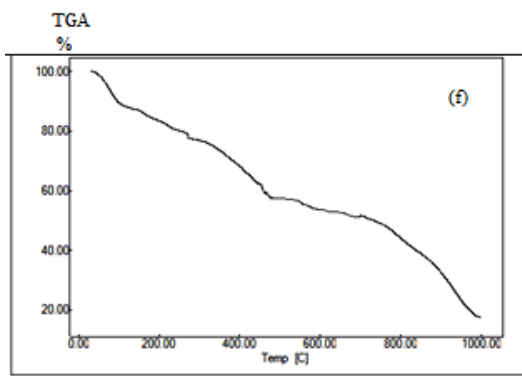
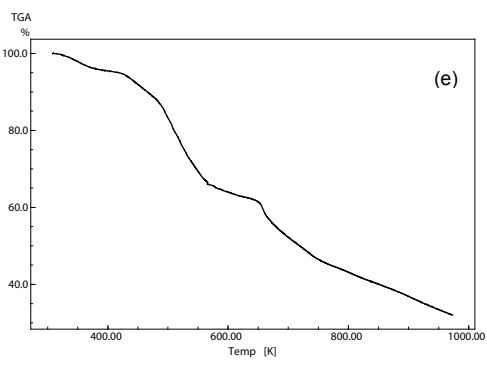
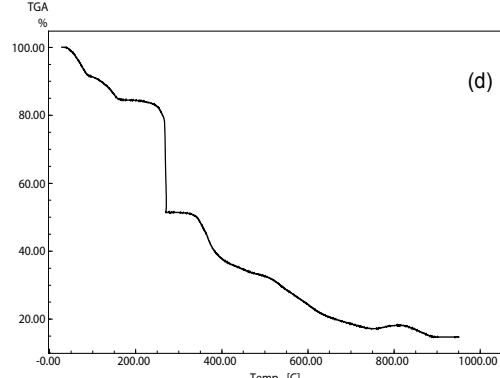
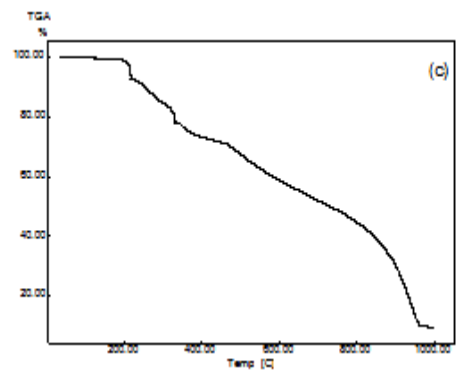
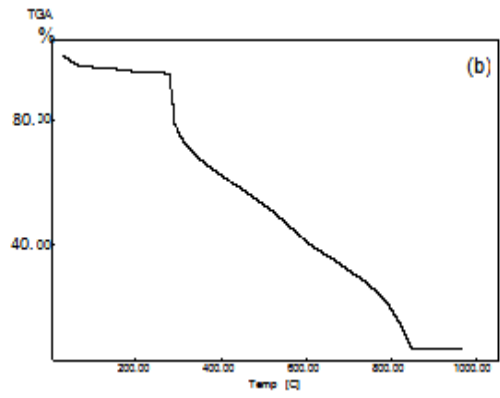
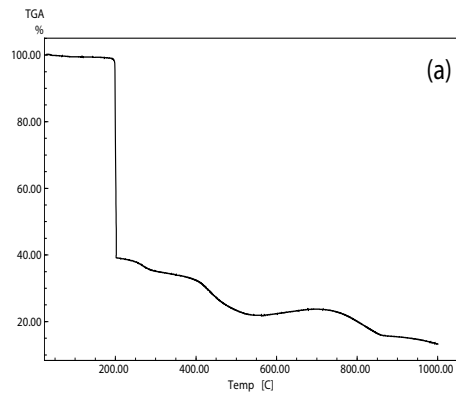
Fig. 1: UV-Vis Spectra of ligands and their metal(II) complexes

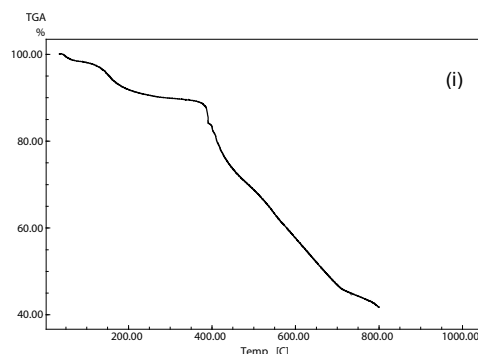
Table 2: The characteristic infrared-absorption band of ligands and their complexes

Sr. No.	Complexes	IR-Absorption band in cm^{-1}							
		$\nu O-H$	$\nu C-H$	$\nu C=O$	$\nu C=N$	$\nu C=C$	$\nu C-O$	$\nu M-N$	$\nu M-O$
L_1	$[C_9H_7NO]$	3213	3074	—	—	1500	1215	—	—
L_2	$[C_7H_7NO_2]$	3209	2974	—	1425	—	—	—	—
1	$[C_{14}H_{12}CuN_2O_4]$	—	3016	—	1599	1446	1545	476	596
2	$[C_{18}H_{12}CuN_2O_2]$	3381	2708	1726	1498	1469	1139	403	525
3	$[C_{16}H_{12}CuN_2O_3]$	—	3012	—	1599	1475	1597	466	518
4	$[C_{14}H_{12}Ni_2NiO_4]$	—	3059	1643	1552	1444	1251	426	508
5	$[C_{18}H_{12}NiN_2O_2]$	—	3062	—	1500	1487	1234	450	505
6	$[C_{16}H_{12}NiN_2O_3]$	—	2955	1639	1520	1410	1200	465	504
7	$[C_{14}H_{12}CoN_2O_4]$	—	3066	1649	1545	1469	1251	410	493
8	$[C_{18}H_{12}CoN_2O_2]$	—	3059	1602	1542	1423	1238	462	505
9	$[C_{16}H_{12}CoN_2O_3]$	—	2955	1600	1639	1420	1255	450	619

Table 3: Thermoanalytical results TGA of Complexes

Sl. No.	Complexes	Decomposition stages	Temp. range °C	Weight loss Found (Cal.) %	Decomposition assignment	Residue found (Cal.) %
1	[C ₁₄ H ₁₂ CuN ₂ O ₄]	Stage-1 Stage-2	198.59-207.59 428.208-607	59.46(60.15) 16.74(19.43)	-C ₁₂ H ₁₂ O ₂ , -N ₂ -C ₂ H ₂	CuO CuO
2	[C ₁₈ H ₁₂ CuN ₂ O ₂]	Stage-1	281.90-847.03	81.96(82.53)	-C ₁₈ H ₁₂ N ₂ O ₂	CuO
3	[C ₁₆ H ₁₂ CuN ₂ O ₃]	Stage-1	213.47-951.69	88.38(88.50)	-NO, -C ₁₆ H ₁₄ NO	CuO
4	[C ₁₄ H ₁₂ N ₂ NiO ₄]	Stage-1 Stage-2	135.12-176.05 253.14-267.18	14.67(15.62) 30.99(31.085)	-N ₂ H ₂ [O] -C ₇ H ₃	NiO NiO
5	[C ₁₈ H ₁₂ NiN ₂ O ₂]	Stage-3	355.24-730.32	35.87(36.05)	-C ₇ H ₂ O	NiO
6	[C ₁₆ H ₁₂ NiN ₂ O ₃]	Stage-1	311.27-989.38	81.30(83.07)	-C ₁₈ H ₁₂ N ₂ O ₂	NiO
7	[C ₁₄ H ₁₂ CoN ₂ O ₄]	Stage-1 Stage-2	178.09-887.21 199.93-202.94	85.94 (86.78) 59.167(60.23)	C ₁₆ H ₁₂ N ₂ O -C ₁₂ H ₁₂ O ₂ , -N ₂	NiO CoO
8	[C ₁₈ H ₁₂ CoN ₂ O ₂]	Stage-1 Stage-2	383.33-433.38 112.77-168.55	17.71(20.16) 13.24 (14.15)	-C ₃ H ₂ -NO, 1/2O ₂	CoO CoO
9	[C ₁₆ H ₁₂ CoN ₂ O ₃]	Stage-1 Stage-2	397.56-592.93 109.98-278.69	56.01(57.03) 10.28(10.61)	-C ₁₂ H ₁₁ N -H ₂ O, 1/2 O ₂	CoO CoO
		Stage-2	387.04-401.46	46.052(47.76)	-C ₇ H ₆ NO	





(a) $[C_{14}H_{12}CuN_2O_4]$; (b) $[C_{18}H_{12}CuN_2O_2]$; (c) $[C_{16}H_{12}CuN_2O_2]$; (d) $[C_{14}H_{12}N_2NiO_4]$; (e) $[C_{18}H_{12}NiN_2O_2]$; (f) $[C_{16}H_{12}NiN_2O_2]$; (g) $[C_{14}H_{12}CoN_2O_4]$; (h) $[C_{18}H_{12}CoN_2O_2]$; (i) $[C_{16}H_{12}CoN_2O_2]$.

Fig. 2: Thermogravimetric analysis of the metal complexes, (a) to (i) in the temperature range from 40°C to 1000°C

Table 4: Crystal data of the mixed ligands complexes of Co(II), Ni(II) and Cu(II)

Chemical formula	$[C_{16}H_{12}CoN_2O_2]$	$[C_{16}H_{12}NiN_2O_2]$	$[C_{16}H_{12}CuN_2O_2]$
Formula weight	339.21	338.97	343.83
Crystal color	Chocolate Brown	Dark Olive Green	Green
Temperature (K)	298	298	298
Wavelength (Å) 0	1.54050	1.54051	1.540598
Radiation	Cu K α	Cu K α	Cu K α
Crystal system	Monoclinic	Orthorhombic	Monoclinic(I)
Space group	P21/a (14)	Pbna(60)	P21/n(14)
A	1.4276	0.7806	0.7515
C	0.9396	1.2891	0.3915
Z	4	8	4
a (Å)	13.819(2)	11.883(3)	13.185(7)
b (Å)	9.68(2)	15.222(4)	17.546(8)
c (Å)	9.095(5)	19.623(6)	6.871(3)
α	90.00	90	90.00
α ()	105.83	90	107.01
\tilde{a} ()	120.00	90	120.00
a/b	0.7449	0.7757	0.7388
c/b	0.5245	0.6056	0.3916
Volume (Å ³)	1170.48	3549.47	1520.03
Dx (g/cm ³)	1.891	1.509	1.738

(ν_2) and ${}^3A_2g \rightarrow {}^3T_2g(p)$ (ν_3) transitions respectively. This spectral bands indicate the complex was square planar geometry. The complexes like C: $[C_{18}H_{12}NiN_2O_2]$, E: $[C_{14}H_{12}N_2NiO_4]$, shows absorption at 598nm, 445nm and 250nm, 595nm, 443nm and 275nm respectively.

The electronic spectral band for L: $[C_{16}H_{12}CoN_2O_3]$ exhibited two characteristic absorption bands of complex at 475nm and 418nm. The complex J: $[C_{18}H_{12}CoN_2O_2]$ and K: $[C_{14}H_{12}CoN_2O_4]$ were showed two characteristic absorption bands at the 570 nm, 435nm and 562nm, 440nm respectively

corresponding to ${}^4T_{1g}(F) \rightarrow {}^4T_{2g}(F)(\nu_1)$; ${}^4T_{1g}(F) \rightarrow {}^4T_{1g}(P)(\nu_2)$. These bands were the characteristics of square planar Co (II) complexes.

The magnetic susceptibility measurements of the complex in the solid state was determined by Gouy balance using Hg $[\text{Co}(\text{SCN})_4]$ as a calibrate. The magnetic moment of Cu (II)-complexes like $[\text{C}_{14}\text{H}_{12}\text{CuN}_2\text{O}_4]$, $[\text{C}_{16}\text{H}_{12}\text{CuN}_2\text{O}_2]$, $[\text{C}_{16}\text{H}_{12}\text{CuN}_2\text{O}_3]$ has been found to be μ_{eff} 1.83 BM., 1.81BM, 1.79BM indicative of one unpaired electron of Cu(II) ion and suggesting that the square-planar geometry of the complex.^{18,19}

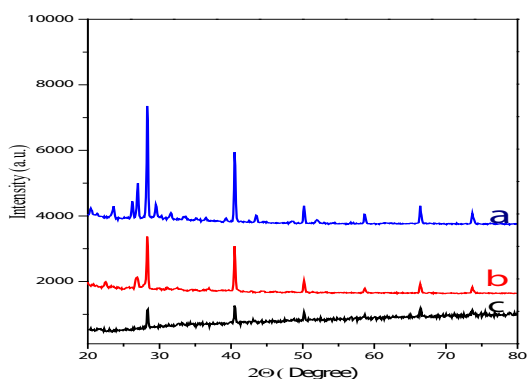


Fig. 3: Powder XRD pattern for nanocrystalline mixed ligand complexes of a) $[\text{C}_{16}\text{H}_{12}\text{NiN}_2\text{O}_2]$, b) $[\text{C}_{16}\text{H}_{12}\text{CuN}_2\text{O}_2]$, c) $[\text{C}_{16}\text{H}_{12}\text{CoN}_2\text{O}_2]$

All the Ni (II) complexes exhibited the diamagnetism phenomenon with square-planar geometry.^{20,21} The magnetic measurement of Co (II) complexes displayed magnetic moment value of 1.87B.M. 2.89BM, 2.34BM. This is due to orbital contribution²².

Conductance measurement

Conductance of the complexes is measured in DMF: H_2O (40:60) solution at a concentration 10^{-4}M ^{23,24}. The low molar conductance values of all metal complexes indicate that the complexes are non-electrolytes²⁵. The results of molar conductance are shown in Table 1.

Thermogravimetric analysis of complexes

Thermogravimetric analysis Fig. 2a to 2i of all the metal complexes was carried out to study the thermal stability and decomposition reaction as a function of time and temperature. In the present investigation, heating rate was suitably controlled at 5°C min^{-1} under non-isothermal way and the weight loss was measured from room temperature to the 1000°C ²⁶. The data is provided with in the Table 3.

The thermogram Fig. 2a for $[\text{C}_{14}\text{H}_{12}\text{CuN}_2\text{O}_4]$ shows that, the thermal decomposition of complex takes place in the temperature range 198.59°C - 207.59°C and is accompanied by a weight loss of 59.46 % as against the calculated weight loss 60.15 %. These weight loss was due to the two phenolic groups and nitrogen gas evolved from the complex. The decomposition step is obtained in

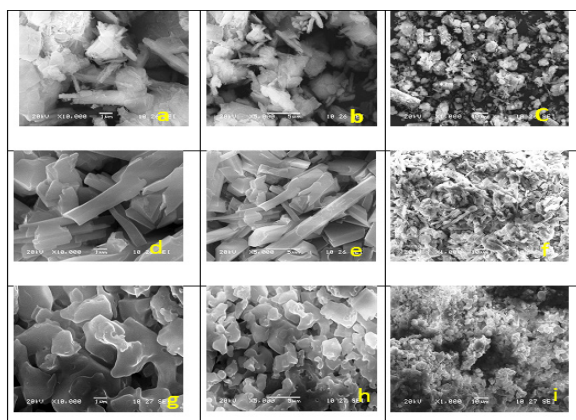


Fig. 4: Scanning Electron Micrographs of Mixed ligand complexes taken on the scale of 1μ , 5μ , 10μ as; a, b, c) SEM image of Co(II) mixed ligands complexes; d, e, f) SEM image of Ni(II) mixed ligands complexes ; g, h, i) SEM image of Cu(II) mixed ligands complexes

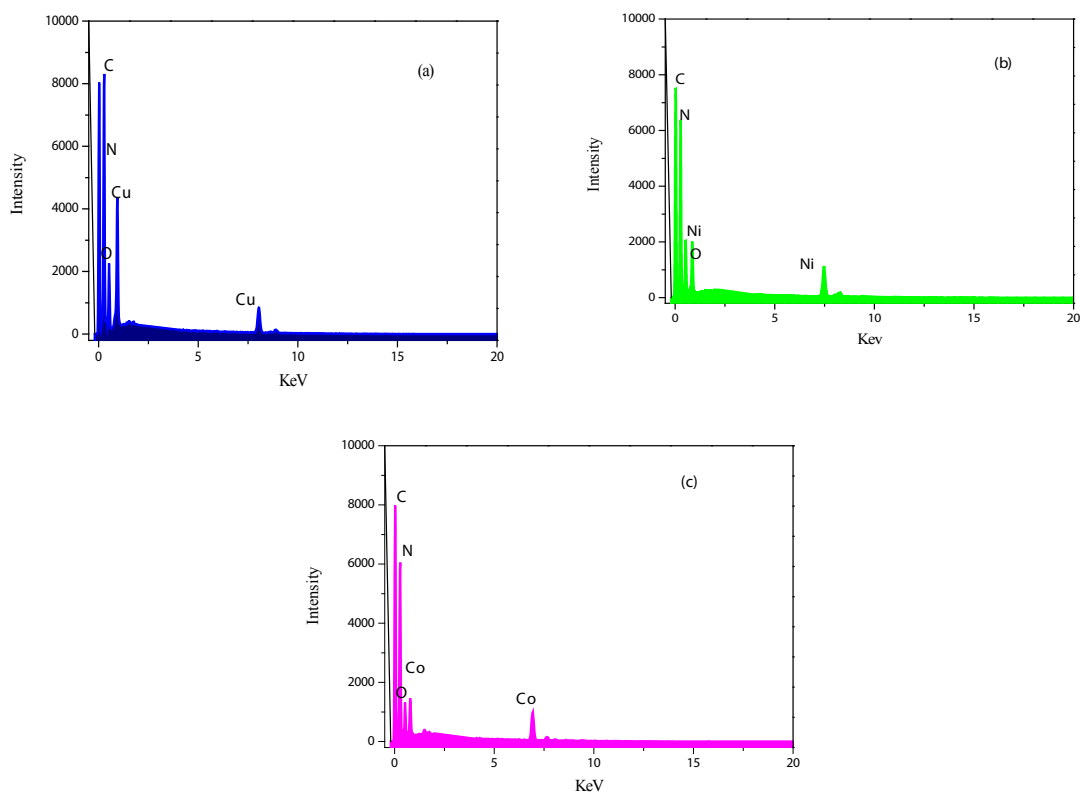


Fig. 5: Electron Dispersive spectrum of nanocrystalline mixed ligand complexes of a) Co (II) , b) Ni(II) and c) Cu(II)

Table 5: Antimicrobial activity measured in Zone of inhibitions

Sr. No.	Complex	Zone of inhibition (mm) for <i>Bacillus subtilis</i>	Zone of inhibition (mm) for <i>E.coli</i>
L1	[C ₉ H ₇ NO]	30	32
L2	[C ₇ H ₇ NO ₂]	15	15
1	[C ₁₄ H ₁₂ CuN ₂ O ₄]	00	00
2	[C ₁₈ H ₁₂ CuN ₂ O ₂]	00	00
3	[C ₁₆ H ₁₂ CuN ₂ O ₂]	15	16
4	[C ₁₄ H ₁₂ N ₂ NiO ₄]	15	16
5	[C ₁₈ H ₁₂ NiN ₂ O ₂]	00	00
6	[C ₁₆ H ₁₂ NiN ₂ O ₂]	17	15
7	[C ₁₄ H ₁₂ CoN ₂ O ₄]	00	00
8	[C ₁₈ H ₁₂ CoN ₂ O ₂]	00	00
9	[C ₁₆ H ₁₂ CoN ₂ O ₂]	16	15
10	[C ₉ H ₇ NO]	00	00

temperature range 428°C to 607°C. This step shows weight loss 16.74 %. This is in accordance with calculated weight loss 19.43 % due to loss of C_2H_2 from the complex. The remaining formation of copper oxide as a residue²⁷.

The thermogram fig. 2b for $[C_{18}H_{12}CuN_2O_2]$ shows that $[C_{18}H_{12}CuN_2O_2]$ shows that its decomposition takes place in temperature range 281.90°C – 847.03°C and is equivalent to loss of two $[C_9H_7NO]$ molecules by weight loss 81.96%, which is in accordance with calculated weight loss 82.53%. The end product, is the formation of CuO residue.

The mixed ligand complex of Cu (II) $-L_1L_2$ shows very interesting result of TG. The decomposition temperature of this complex is in the range 213.43°C -951.69°C, which is in between Cu (L_1) and Cu (L_2) complexes. At the temperature 326.45°C loss of NO group and further decomposition reaction was continue to decompose the organic molecules .The total weight loss of this step is 88.38% which is in accordance to the calculated weight loss 88.50 %. This weight loss is equivalent to the of L_1 and L_2 . The chocolate brown coloured CuO residue was obtained.

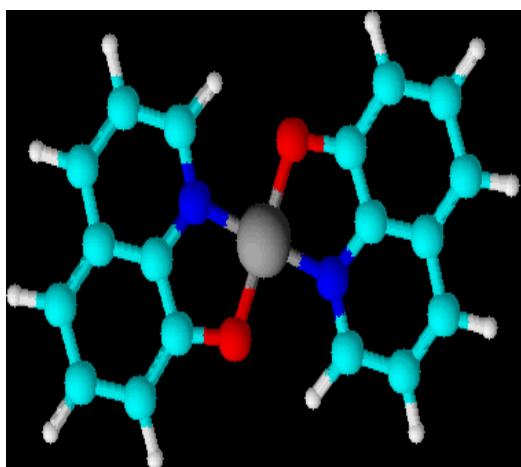
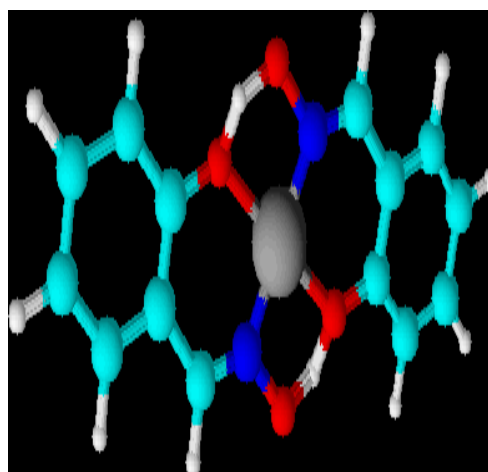
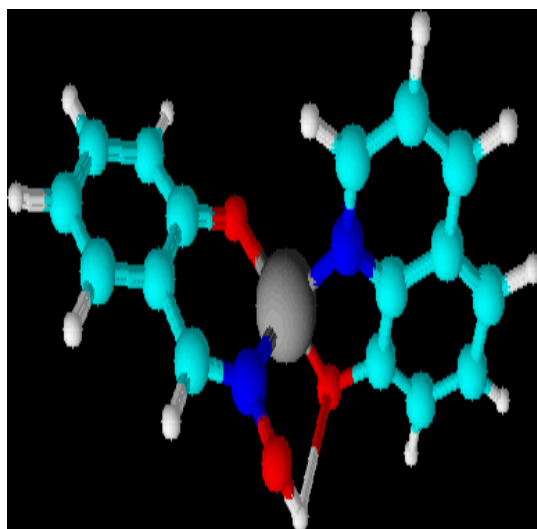
[ML_1][ML_2][ML_1L_2]

Fig. 6: Suggested chemical bonding and 3D-structure for complexes

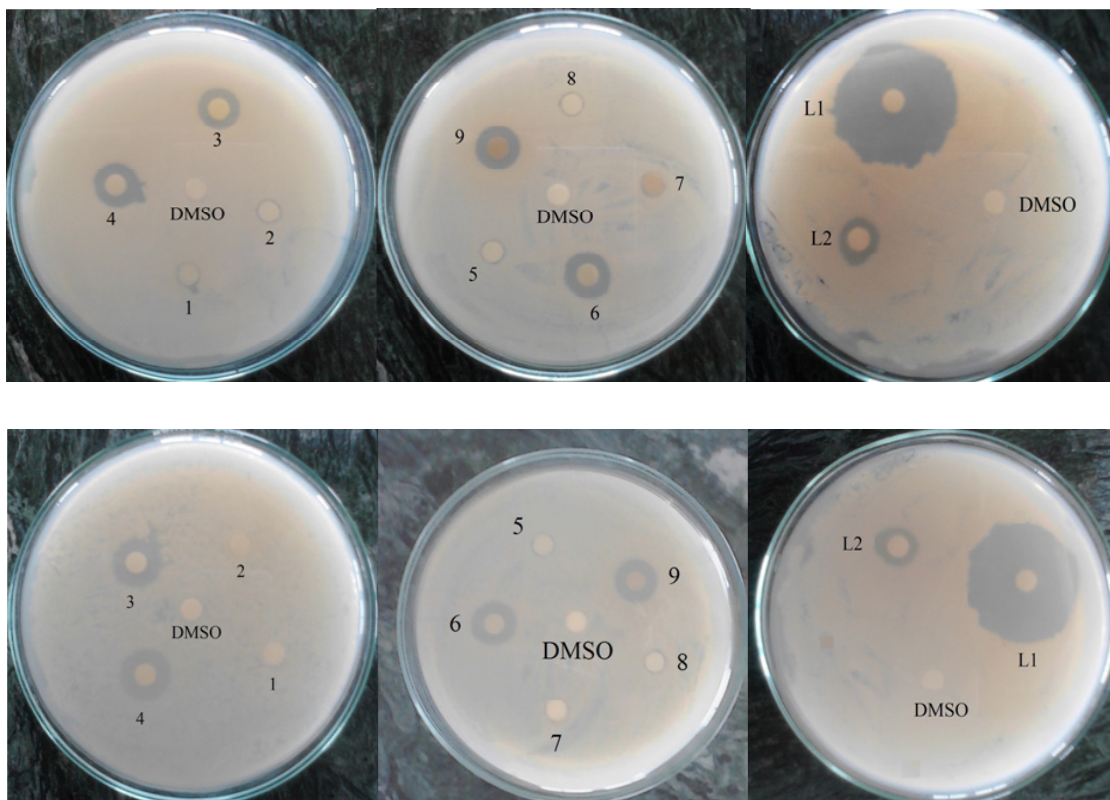


Fig. 7: Photograph of Biological activity of L_1 , L_2 and their metal complexes a) Antimicrobial activity against *Bacillus subtilis* NCIM 2063; b) Antimicrobial activity against *E.coli* NCIM 2341

All the complexes of Ni(II) showed fig. 2d to 2f the final product NiO residue²⁸. The complex $[C_{14}H_{12}N_2NiO_4]$ thermogram shown in fig.2d decomposes in three steps. The weight loss observed was 14.67% in first step, 30.995% in second and 35.87% in the third step at 135.12°C -176.05°C, 253.14°C-267.18°C, 353.24°C - 730.32 °C, with loss N_2H_2O , C_7H_3 , and C_7H_2O groups respectively. The TG of complex $[C_{18}H_{12}NiN_2O_2]$ shows the decomposition of $C_{18}H_{12}N_2O_2$ organic compound at the 311.27°C -989.38°C. The % weight loss was found to be 81.30%. This was attributed to calculate weight loss was 81.07%. The mixed ligand complex of Ni (II) - L_1L_2 decomposed in the temperature range 178.09°C -887.21°C, indicating that complex decomposes with to loss of $C_{16}H_{12}N_2O_2$ molecules. The total weight loss of this step is 85.94% which is in accordance with the calculated weight loss 86.78%.

TG fig. 2g to 2i of all the Co(II) complexes was carried out in N_2 atmosphere with flow rate 50ml/min. and the heating rate was 8°C min⁻¹. The complex $[C_{14}H_{12}CoN_2O_4]$ shows two decomposition steps. The first step (199.93°C - 202.94°C) and the second step (383.33°C -433.38°C) are accompanied by mass loss 59.16 % and 17.71 %, respectively. These first steps may be due to the decomposition of two phenols and one nitrogen molecules. The second step may be due to the loss of $-C_2H_2$ molecule. All the observed weight loss was found to be equal to theoretical weight loss. The complex was converted to metallic oxide as final residue²⁹. TG fig. 2h of $C_{18}H_{12}CoN_2O_2$ showed two decomposition steps in the temperature range 112.77°C to 168.55°C, with 13.24% (14.15%) weight loss, which was attributed to the loss of $NO, 1/2O_2$ moieties. In the second step the percentage weight loss 56.01 % (57.03%) weight loss was observed to loss of $C_{12}H_{11}N$ group of the complex.

The mixed ligand complex of Co(II) shows two decomposition steps one is for loss of Hydrogen gas and two oxygen molecule from the complex³⁰. which were removed by purge gas nitrogen having flow rate 50ml/min. Then the second step was attributed to loss of $[C_7H_7NO_2]$ molecules, and the formation of CoO residue.

X-ray diffraction analysis

The structures of complexes were confirmed by powder XRD recorded at 2θ and $20-80^\circ C$. All the mixed ligand Cu (II), Ni (II) and Co (II) metal ion complexes of show broad and intense peak. The line broadening of the crystalline diffraction peaks in mixed ligands complexes of Co(II), Ni(II) and Cu(II) complexes shows higher crystallinity and fine nanoparticles. The XRD patterns of the mixed ligand complexes are shown in Fig. 3

The unit cell parameters were obtained by using Powder -X software methods. The complexes of mixed ligands of the Cobalt, Nickel and Copper shows Monoclinic (P), Orthorhombic (P)³¹ and monoclinic (I) respectively. [JCPDS: 76-0476, JCPDS 43-1973]. The diffraction data has been summarized in Table 4.

Scanning Electron Microscopy and Electron dispersive Spectroscopy

The complexes were scanned by Scanning Electron Microscope is the good agreements for formation of the nanocrystalline complexes with best morphology. The SEM micrographs of these complexes were taken in the scale of 1 μ m, 5 μ m, and 10 μ m for each nanocrystalline mixed ligands metal complexes. The scanning electron micrograph of the complexes shown in Fig. 4 The complex $[C_{18}H_{12}CuN_2O_2]$ shows the shape like nanoflowers,³² the Co(II) mixed ligand complex shows nanofoil shaped rod with internal hexagonal array²². The Ni (II) mixed ligand complex of N, O donors shows the leaf like morphology. All the mixed ligand complexes have grain size less than 10 nm. The average size of these complexes were calculated by using 2θ , FWHM, and Cu-K α radiation of wavelength 1.54058 Å from powder XRD with grain size measurement programmers software. The nanocrystalline sizes of mixed ligands complexes of Cu (II), Ni (II) and Co (II) are 7.90488nm; 6.83833nm and 7.31095nm respectively. The decrease in the size indicates

the increased surface to volume ratio increases. The SEM study shows good agreement for the formation of nanocrystalline complexes and also supporting tool for the powder XRD. Therefore these complexes can be used as the catalysts in organic transformations.

The Electron dispersive spectra of mixed ligand metal complexes were taken. The sample was coated on the Platinum plates at room temperature. The Electron dispersive spectroscopic studies of mixed ligand metal complexes show compositions of the nanostructured complexes. The EDS analysis data matched with C, H, and N elemental analysis result. The percentage of oxygen in all complexes analyzed by EDS was found to be high due to the oxygen adsorbed on the complexes. The complexes have nanostructures with array of different shapes in which array, the oxygen get adsorbed and percentage of oxygen get elevated. The EDS spectrum is shown in Fig 5.

The data of elemental analysis are shown in Table 1. and EDS were as calculated (found) for the complex are $[C_{16}H_{12}CuN_2O_2]$ C 55.89%(55.71%), N 8.15%(8.04%), O 13.16% (17.77%), Cu 18.48%(18.40%). The complex $[C_{16}H_{12}NiN_2O_3]$ contain was C 55.69 % (55.56%), N 8.16%(8.13%), O 14.16% (17.02%), Ni 17.32%(17.15%) and the mixed ligands complex of Cobalt as $[C_{16}H_{12}CoN_2O_3]$ C 56.65%(56.66%), N 8.26%(7.64), O 14.15 (16.98), Co 17.37% (17.22%). The possible 3D-chemical structures homoleptic $[ML_1]$, $[ML_2]$ and heteroleptic $[ML_1L_2]$ complexes were shown in fig. 6

Antimicrobial activity of Complexes and Ligands

The result of antimicrobial activity of the synthesized complexes and ligands photo are shown in Fig.7.

The complexes 3: $[C_{16}H_{12}CuN_2O_2]$, 4: $[C_{14}H_{12}N_2NiO_4]$, 6: $[C_{16}H_{12}NiN_2O_2]$, 9: $[C_{16}H_{12}CoN_2O_2]$ showed antimicrobial activity against both *B. subtilis* NCIM 2063 and *E.coli* NCIM 2341. All other complex is inactive against test organism. Both ligands L_1 : $[C_9H_7NO]$ and L_2 : $[C_7H_7NO_2]$ showed antimicrobial effect. The L_1 : $[C_9H_7NO]$ shown larger zone than L_2 : $[C_7H_7NO_2]$ ³³. In case of heteroleptic complexes of Cu(II), Co(II) and Ni(II) shows high antimicrobial

activity as compared to the homoleptic complexes. The antimicrobial activity of all the Ligands and complexes were summarized in Table 5.

CONCLUSION

The mixed ligands complexes of two N, O donor ligands were successfully synthesized and characterized by different spectral techniques and micro analytical methods. The synthesized mixed ligand complexes were nanocrystalline in nature with good morphology. All complexes have shown non-electrolytic behavior as observed from the conductance measurement. The powder XRD, SEM gives the result of formation of crystalline fine nanoparticles. The nanocrystalline mixed ligand complexes has the less than 10nm therefore these

complexes may be used as catalyst in synthetic organic chemistry for functional group transformation. The nanocrystalline heteroleptic complexes show higher antimicrobial activity than other complexes. Among complexes $[C_{16}H_{12}CuN_2O_2]$, $[C_{14}H_{12}N_2NiO_4]$, $[C_{16}H_{12}NiN_2O_2]$, $[C_{16}H_{12}CoN_2O_2]$ have shown antimicrobial activity. Both ligands showed positive results. But activity of $L_1: [C_9H_7NO]$ was nearly double than $L_2: [C_7H_7NO_2]$.

ACKNOWLEDGMENTS

The authors are very grateful to management of Ahmednagar Jilha Maratha Vidya Prasarak Samaj's, Principal Dr.B.H.Zaware, New Arts Commerce and Science College Ahmednagar for providing laboratory facilities.

REFERENCES

- Milios CJ, Stamatatos TC, Perlepes SP, *Polyhedron*, **2006**, *25*, 134-194.
- Babu MSS, Krishna PG, Reddy KH, Philip GH, *Indian J. Chem.*, **2008**, *47*, 1661-1665.
- R. Prasad, M. Mathur, *J. Serbian Chem. Soc.*, **2002**, *67*, 825-832.
- B. Khera, A. K. Sharma, N. K. Kaushik, *Polyhedron*, **1983**, *2*, 1177-1180.
- M. Kurtoglu, *J. Serbian Chem. Soc.*, **2010**, *75*, 1231-1239.
- Raptopoulou CP, Sanakis Y, Boudalis AK, Psycharis V. *Polyhedron*, **2005**, *24*, 711-721.
- Aggarwal RC, Singh NK, Singh RP, *Synth. React. Inorg. Met. Chem.*, **1984**, *14*, 637-650.
- Patel KD, Patel HS, *A.J. of chem.* **2013**, <http://dx.doi.org/10.1016/j.arabjc.2013.03.019>.
- Masalovich MS, Ardasheva LP, Shagisultanova G, *Zh. Neorg. Khim.*, **2006**, *51*, 1591-1596.
- Thakkar N V., Thakkar JR., *Synth. React. Inorg. Met. Chem.*, **2000**, *30*, 1871-1887.
- Prasad RV, Thakkar NV., *J. Mol. Catal.*, **1994**, *92*, 9-20.
- Angelusiu MV, Barbuceanu SF, Draghici C, Almajan GL. *Almajan. Eur. J. Med. Chem.*, **2010**, *45*, 2055-2062.
- Hartophylles M., *Zeitschrift fur anorganische und allgemeine Chemie*, **1995**, *621*, 645-653.
- Sallam SA., *Transit. Met. Chem.*, **2006**, *31*, 46-55.
- Alemi AA, Shaabani B, B. Shaabani, *Acta Chim. Slov.*, **2000**, *47*, 363-369.
- Baran EJ., *Zeitschrift fur Naturforsch. - Sect. B J. Chem. Sci.*, **2005**, *60*, 663-666.
- Cupertino D, Mcpartlin M, Zissimos AM, **2001**, *20*, 3239-3247
- Downing RS, Urbach FL, *J. Am. Chem. Soc.*, **1969**, *91*, 5977-5983.
- Patil SS, Thakur GA, Shaikh MM., *ISRN Pharm.*, **2011**, *2011*, 1-6.
- Cristóvão B., *J. Serbian Chem. Soc.*, **2011**, *76*, 1639-1648.
- Jain SK, Garg BS, Yudhvirk, **1987**, *77*, 73-77.
- Ibrahim KM, Bekheit MM., *Transit. Met. Chem.*, **1988**, *232*, 230-232.
- Li H, Li Y., *Nanoscale*, **2009**, *1*, 128-132.
- Firenze UDI, *Inorg. Chem.*, 1966, *5*, 1960-1963.
- Raman N, Ravichandran S, Thangaraja C, *J. Chem. Sci.*, **2004**, *116*, 215-219.
- Turkoglu O, Soylak M, Belenli I., *Collect. Czechoslov. Chem. Commun.*, **2003**, *68*, 1233-1242.
- Mohamed GG, El-wahab ZHA., **2003**, *73*, 347-359.

28. Mashaly MM, Abd-Elwahab ZH, Faheim AA., *J. Chinese Chem. Soc.*, **2004**, *51*, 901–915.
29. Abdallah SM, Zayed MA, Mohamed GG, *Arab. J. Chem.*, **2010**, *3*, 103–113.
30. Nayak SC, Das PK, Sahoo KK., *Chem. Pap.*, **2003**, *57*, 91–96.
31. Patel KS, Patel JC, Dholariya HR, Patel VK, Patel KD, **2012**, *2012*, 49–59.
32. Liu B, Zhu S, Zhang W, Chen C, Zhou Q, Q. Zhou, **2007**, *entry 10*, 5834–5835.
33. Shao Q, Wang T, Wang X, Chen Y. Chen, *Front. Optoelectron. China*, **2011**, *4*, 195–198.
34. Bagihalli GB, Avaji PG, Patil SA, Badami PS, *Eur. J. Med. Chem.*, **2008**, *43*, 2639–2649.